ARTICLE

New 2-cyanobenzyl-nitrile-dithiolate to di-*n*-butyltin(IV)-*bis*-(1-alkoxy-isoquinoline-4-nitrile thiolate): Crystallographic and Computational Studies

Received 00th January 20xx,
Accepted 00th January 20xx

DOI: 10.1039/x0xx00000x

Amita Singh,[a,b] Ayushi Singh,[b] Devyani Srivastava,[b] Gabriele Kociok-Köhn,[c] Randolf D. Köhn,*[d] Abhinav Kumar*[b] and Mohd. Muddassir[e]

The reaction between di-*n*-butyltin(IV) chloride with the dinegative dithiolate ligand 2-(cyanobenzo)nitrile-dithiolate in two different alcoholic media *viz.* methyl alcohol and ethyl alcohol fortuitously yielded di-*n*-butyltin(IV)-*bis*-(1-methoxy-isoquinoline-4-nitrile thiolate) (**Sn-Me**) and di-*n*-butyltin(IV)-*bis*-(1-ethoxy-isoquinoline-4-nitrile thiolate) (**Sn-Et**). Similarly the reaction of di-*n*-butyltin (IV) chloride with 2-methoxy phenyl acetonitrile dithiolate yielded di-*n*-butyltin(IV)-2-methoxy phenyl acetonitrile dithiolate (**2-MeCN-Sn**) . These compounds have been characterized by micro analyses, IR, UV-Vis, ^{1}H, ^{13}C and ^{119}Sn NMR spectroscopy as well as by single crystal X-ray diffraction technique in case of **Sn-Et, Sn-Me**. The X-ray analyses revealed that in both **Sn-Me** and **Sn-Et,** the Sn(IV) center adopts a skew trapezoidal bipyramidal geometry with Sn at the centre and two sulfur and two ring nitrogen atoms of 1-alkoxy-isoquinoline-4-nitrile thiolates are at the corners of a trapezoid with two n-butyl groups adopting axial positions resembling the *cis-trans* pathway. Both **Sn-Me** and **Sn-Et** display varied types of non-covalent interactions. The nature of these interactions has been addressed with the aid of Hirshfeld surface analysis, density functional theory and quantum theory of atoms-in-molecules (QTAIM) analyses.

Introduction

Ligands containing sulfur donors are gaining consideration amongst inorganic and materials chemists because of their diverse complexation ability, ease of syntheses, efficient π-electron delocalization and their variety of metal-ligand linkage ability.[1-5] Several classes of dithiolates, *viz*. dithiocarbamates,[6a,b] xanthates,[6c,d] dithiophoshonates and dithiophosphinates,[6e,f] are gaining attention as they engender targeted metallic/organometallic complexes. In addition, some thiolates comprising of N, O donors *viz.* thiosemicarbazones, [7a] semicarbazones,[7b, 7c] and dithiocarbazates,[7d,7e] and their metal complexes are also being investigated by inorganic chemists and crystal engineers as they can yield interesting tuned supramolecular frameworks.[7,8] By choosing apt designing strategies, these systems could be explored as interesting supramolecular assemblies to achieve desirable properties.[8]

Amongst a plethora of sulfur-based coordination complexes, the chemistry of compounds bearing Sn–S bonding had drawn immense attention because such class of compounds display interesting properties and supramolecular architectures.[1-8] Also, complexes comprising Sn-S, the Sn-N, Sn-O bonds display several advantages over other main group compounds.[6-15] This is because of the inherent Lewis acidity of Sn(IV) which forms stable bonds with these heteroatoms.[6-15] In addition to supramolecular assemblies, such class of compounds finds application in the fields of medicine and pharmacology, which is due to the distinct stereogenic property of the Sn(IV) center which could be attuned by introducing modifications in ligand structure.[9]

In addition to normal Sn-based coordination complexes, the organotin thiolate/dithiolates are still gaining attention amongst as single source precursors (SSPs) for tin sulfides. [10, 11] Their complexes and appropriate sulfides are used as catalytic agents,[12] as thin films of organotin(IV) in optoelectronics in solar energy,[13] and sensors for anions (sensor/receptor). Apart from these, main group thiolate based complexes are also reported which find applications in material science and exhibit imperative biological activities.[16]

There are numerous reports which describe organotin(IV) complexes coordinated to monoanionic dithio ligands. However, reports dealing with organotin(IV) complexes coordinated to dianionic dithiolates are scarce.[17] In view of this, we recently reported a series of new 1D coordination polymers containing diorganotin(IV) moieties coordinated to a dinegative dithiolate ligand derived from benzylcyanide amongst which the dimethyltin(IV) dithiolate displayed interesting C···Sn tetrel bonding.[18]

[a] *Department of Chemistry, Dr. Ram Manohar Lohiya Avadh University, Ayodhya 224 001, India*
[b] *Department of Chemistry, Faculty of Science, University of Lucknow, Lucknow 226 007, India. Email: abhinavmarshal@gmail.com*
[c] *Materials and Chemical Characterisation Facility (MC2), University of Bath, Claverton Down, Bath, BA2 7AY, UK.*
[d] *Department of Chemistry, University of Bath, Calverton Down, Bath, BA2 7AY, UK Email: chsrdk@bath.ac.uk*
[e] *Department of Chemistry, College of Sciences, King Saud University, Riyadh 11451, Saudi Arabia*
[f] *Electronic Supplementary Information (ESI) available: See DOI: 10.1039/x0xx00000x*

Hence, to further extend this work and in our continuous pursuit to engender newer supramolecular architectures in new diorganotin(IV) complexes with dinegative dithiolate ligands we sought to react di-*n*-butyltin(IV) dichloride with another dianionic dithiolate ligand derived from 2-(cyanomethyl)benzonitrile. Fortuitously, instead of giving the expected normal product, the reaction yielded di-*n*-butyltin(IV)-*bis*-(1-methoxy-isoquinoline-4-nitrile thiolate) (**Sn-Me**) and di-*n*-butyltin(IV)-*bis*-(1-ethoxy-isoquinoline-4-nitrile thiolate) (**Sn-Et**), wherein the dinegative ligand 2-(cyanobenzo)nitrile-dithiolate underwent cyclisation to 1-methoxy-isoquinoline-4-nitrile thiolate and 1-ethoxy-isoquinoline-4-nitrile thiolate in the presence of methyl alcohol and ethyl alcohol, respectively as well as di-*n*-butyltin(IV) additionally 2-methoxy phenyl acetonitrile dithiolate yielded di-*n*-butyltin(IV)-2-methoxy phenyl acetonitrile dithiolate (**2-MeCN-Sn**). The newly synthesized compounds displayed a peculiar molecular framework and exhibited interesting supramolecular architectures employing variety of non-covalent interactions. The natures of these interactions have been addressed with the aid of different computational tools. The pertinent outcomes of this investigation is presented herewith.

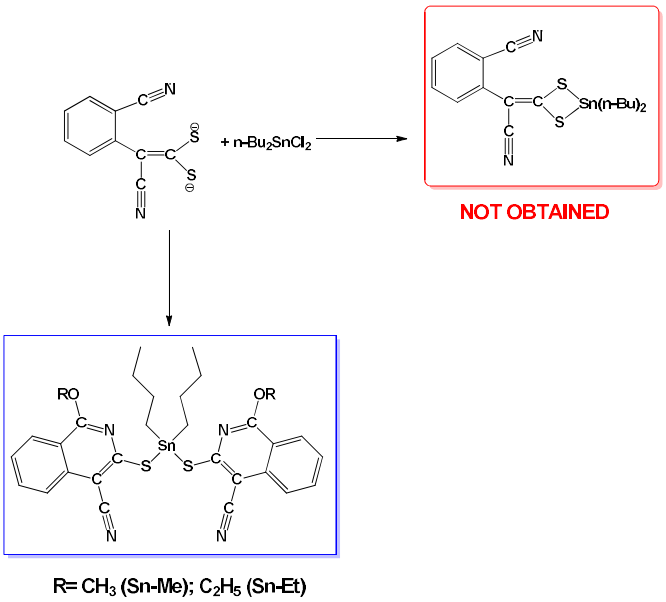

Scheme 1. Synthetic routes for the preparation of complexes.

Results and Discussion

Syntheses

The dianionic ligand 2-cyanobenzyl-nitrile-dithiolate was prepared by reacting 2-(cyanomethyl)benzonitrile with potassium hydroxide and carbon disulfide in appropriate stoichiometric ratio. Addition of a dichloromethane solution of di-n-butyltin(II) dichloride into methanol/ethanol solution of 2-cyanobenzyl-nitrile-dithiolate in 1:1 stoichiometric ratio yielded the unexpected complexes (Scheme 1).

The unexpected products were obtained in low yield and the alcohol solvent was observed to be involved in their formation. In the first step, one-half equivalent of di-*n*-butyltin(IV) chloride coordinated in monodentate mode to one of the negatively charged sulfur atoms of the dithiolate ligand and the cyano nitrogen attacks the dithiolate carbon atom which eliminated n-Bu_2SnS and Cl^- as by-products. The attack of alcohol oxygen to the electron deficient cyano carbon atom with concomitant liberation of H^+ resulted in the cyclized thiolate ligand followed by di-n-butyltin(IV) chloride coordination to yield the final product (Scheme 2). In our previous report where benzylcyanide ditihiolate was reacted with di-n-butyltin(IV) chloride yielded the expected one dimensional coordination polymers of organotin.[18] Additionally, an analogous dithiolate ligand having $–OCH_3$ group at *o*–position to (CN)C=CS_2 was synthesized and reacted with n-Bu_2SnCl_2, that yielded the anticipated product similar to benzylcyanide dithiolate (Scheme S1) that had been characterized spectroscopically.[18] This suggest that, the presence of *o*-CN at the aromatic ring in dithiolate is playing vital role in cyclization. Apart from this, the attainment of six membered aromatic ring to engender *iso*-quinoline moiety may be the driving force for this reaction. Both unexpected products **Sn-Me** and **Sn-Et** and **2-MeCN-Sn** were air and moisture stable and have been characterized by microanalyses, FTIR and multinuclear NMR spectroscopic techniques and their structure was determined by single crystal X-ray diffraction techniques.

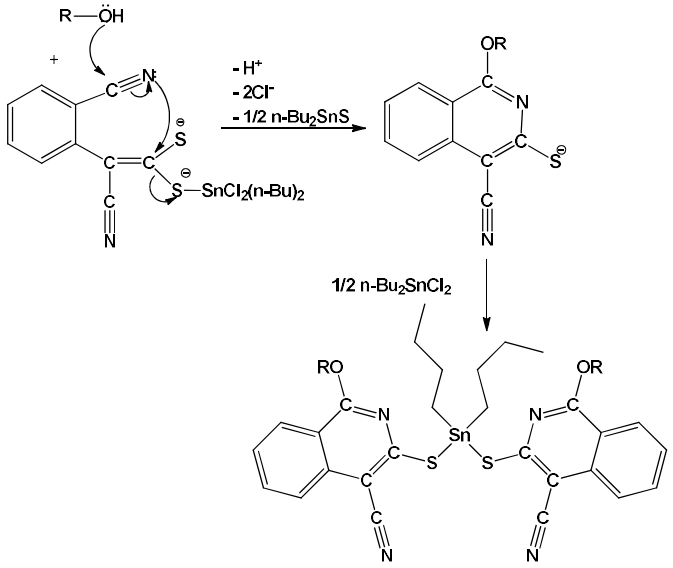

Scheme 2. Plausible mechanistic pathway for the formation of the unexpected product.

Spectroscopy

In FTIR spectra of both **Sn-Me** and **Sn-Et**, bands appearing at ~1550-1600 and 1100-1125 cm^{-1} could be attributed to $\nu_{C\equiv N}$ and ν_{C-S}, respectively and strong bands at 3400 and 3269 cm^{-1} confirmed the presence of an aromatic ring comprising nitrogen. To confirm the purity and composition of **Sn-Me** and **Sn-Et**, **2-MeCN-Sn** ^{1}H NMR spectroscopy has been performed. In three complexes, resonances matched well with the

corresponding hydrogens of the cyclized ligand and 2-methoxy phenyl acetonitrile dithiolate ligand and n-butyl group of organotin(IV). The signals in the region of δ 8.19-6.99 ppm indicate the presence of deshielded aromatic rings, while peaks at δ 4.13 have confirmed the presence of O-CH_3 group in **Sn-Me**. Similarly, in **Sn-Et** the two signals between δ 4.41-4.52 confirmed the presence of O-C_2H_5 group, and δ 6.99 indicated the presence of O-CH_3 group in **2-MeCN-Sn** . In the ^{13}C NMR spectra of **Sn-Me** and **Sn-Et, 2-MeCN-Sn** the signal at δ 195.8 and 194.3 and at δ 198.8 is suggestive of the C-S (thiolate), moiety and the signals appearing at δ 123.0 correspond to the cyano group. In addition, signals between 33-58 ppm confirmed the presence of the CH_3 and CH_2 unit of the –OMe and –OEt, groups. Further, in the ^{119}Sn NMR spectra for three compounds, the appearance of only one signal confirmed the existence of Sn(IV) in only one chemical environment and the position of signals at around δ -137.9 and -140.2, indicated the presence of a penta-coordinated dibutyltin (IV) moieties in both **Sn-Me** and **Sn-Et**, respectively.[18-20]

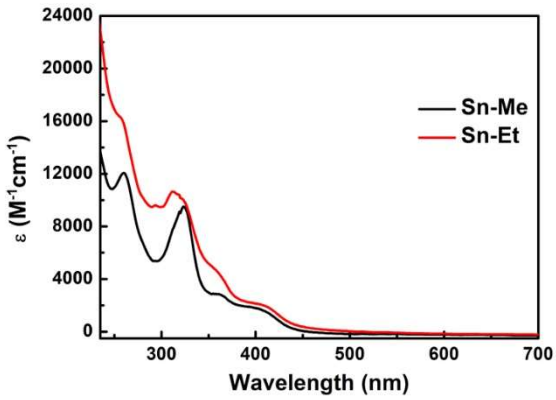

Fig. 1 Electronic absorption spectra for **Sn-Me** and **Sn-Et** recorded in 1× 10^{-5} M ethanol solution.

Electronic absorption spectroscopy for both **Sn-Me** and **Sn-Et** recorded in ethanol displayed three prominent bands (Fig. 1). The band at ~407 nm originates from ligand-to-ligand transitions between the two thiolate ligands.[21] Bands at ~250 nm and ~320 nm originate from intraligand charge transfer.[21] Also, unlike transition metal complexes, no band corresponding to Sn(IV) was observed.

Molecular Structure Description

Crystals suitable for X-ray diffraction analysis were obtained by slow evaporation of methanol and ethanol solutions of **Sn-Me** and **Sn-Et**, respectively. Both compounds crystallize in the monoclinic space group $P2_{1/c}$ with four molecules in their respective unit cells. In both **Sn-Me** and **Sn-Et**, the Sn(IV) center adopts a skew trapezoidal bipyramidal geometry where the Sn is at center and two sulfur centers S1 and S2 as well as two ring nitrogen centers N2 and N4 are at corners of the trapezoid (Fig. 2). In skew trapezoidal bipyramidal geometries for *cis*-diorganotin(IV) compounds the ∠C-Sn-C bond angles exist basically in the range between 102–110°, while for the trans isomer the respective range is between 145-180°.[22] The two n-butyl groups adopt axial positions subtending the C1-Sn-C5 angle of 133.4(4)° and 134.49(13)° for **Sn-Me** and **Sn-Et**, respectively resembling the *cis-trans* pathway (Fig. 2). The two strong Sn-S bonds *viz.* Sn-S1 and Sn-S2 are 2.4766(19) Å, 2.463(2) Å, respectively for **Sn-Me**, while for **Sn-Et** they are 2.4694(18) Å and 2.4790(8) Å. These two strong Sn-S bonds adopt *cis* orientation with respect to each other subtending an acute angle of S1-Sn-S2 of 92.99(7)° and 92.52(3)° for **Sn-Me** and **Sn-Et**, respectively. The Sn-N2 and Sn-N4 interaction distances in **Sn-Me** are 2.866(2) Å and 2.840(2) Å, respectively and in **Sn-Et**, these distances are 2.891(2) Å and 2.767(2) Å, respectively. The weaker Sn···N interaction with the N2-Sn-N4 angle of 147.38(4)° and 147.57(7)° are ~32° less from being co-linear for **Sn-Me** and **Sn-Et**, respectively. Also, the Sn···N interactions are longer than the sum of the covalent radii of the tin and nitrogen (2.10 Å) but significantly below the sum of the van der Waals radii of these atoms (3.72 Å).[22] These geometrical parameters are in line with previously reported organotin thiolates and dithiolates.[3, 4]

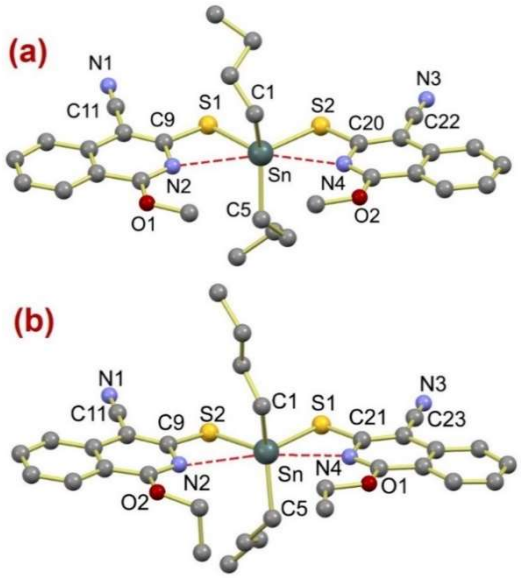

Fig. 2 Perspective view of (a) **Sn-Me** and (b) **Sn-Et**. (H atoms and disordered alkyl fragments have been removed for clarity.)

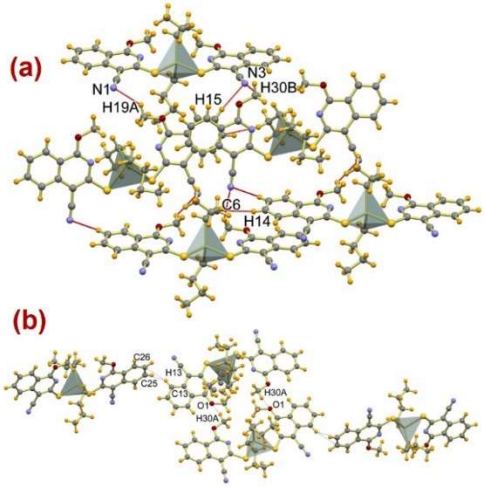

Fig. 3 Supramolecular architecture of **Sn-Me** stabilized by (a) C≡N···H and C···H; (b) O···H and C-H···π interactions.

The supramolecular architecture of **Sn-Me** is stabilized by several weak C≡N···H, C···H, O···H and C-H···π non-covalent interactions (Fig. 3). The C≡N1···H19A interaction is 2.48 Å long while C≡N3 exhibit bifurcated C≡N3···H interactions with –OCH_3 hydrogen H30B and aromatic hydrogen H15 with C≡N3···H15 and C≡N3···H30B distances of 2.68 and 2.64 Å, respectively (Fig. 3a). Apart from these interactions, **Sn-Me** displays intermolecular C-O1···H30A interaction of 2.61 Å in antiparallel mode to generate a dimer which further subtends to engender C-H···π interactions formed between aromatic hydrogen H13 with aromatic carbon C25 and C26. The C-H···C25 and C-H···C26 distances are 2.82 and 2.76 Å (Fig. 3b).

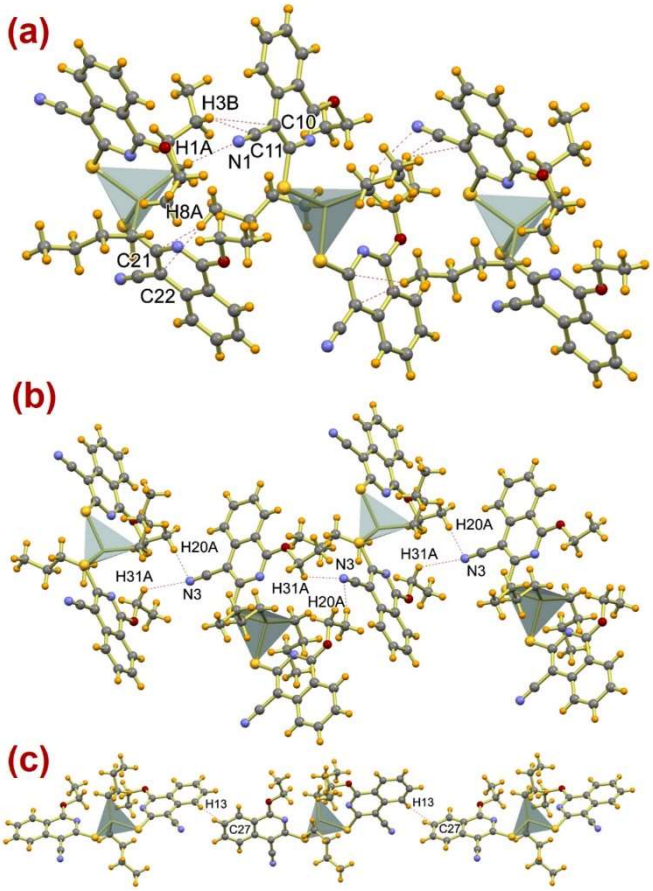

Fig. 4 Supramolecular architecture of **Sn-Et** stabilized by (a) C≡N···H, C-H···π and C···H; (b) Bifurcated C≡N···H and (c) C-H···π interactions.

In **Sn-Et**, the supramolecular framework is stabilized by several weak C≡N···H, C-H···π and C···H non-covalent interactions (Fig. 4). The C11≡N1···H1A interaction is 2.71 Å long and the C10···H3B and C11···H3B interactions are of 2.85 and 2.63 Å length, respectively (Fig. 4a). The methyl hydrogen of the n-butyl group is engaged in forming C-H···π interactions with the C21 and C22 carbon of the heteroaromatic ring with C-H···C21 and C-H···C22 distances of 2.81 and 2.79 Å, respectively (Fig. 4a). As in **Sn-Me**, bifurcated C≡N3···H20A and C≡N3···H31A interactions exist in **Sn-Et** with weak interaction distances of 2.60 and 2.72 Å, respectively (Fig. 4b). Apart from these interactions, **Sn-Et** displays intermolecular C-H13···C27 interaction of 2.81 Å length to generate a 1D supramolecular chain (Fig. 4c).

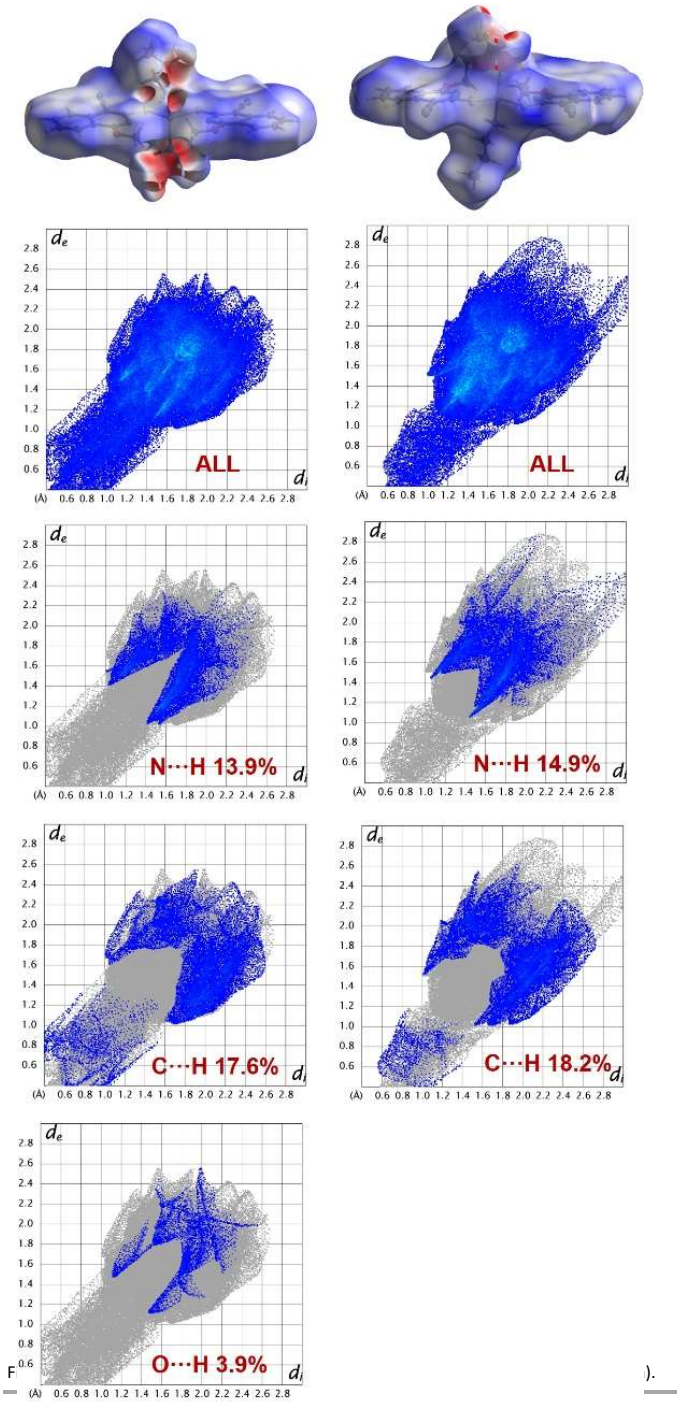

F).

Hirshfeld surface analyses

Hirshfeld surface analyses for both **Sn-Me** and **Sn-Et** have been performed, which depict dominant interactions as circular depressions in their respective d_{norm} plots constructed between -0.5 to 1.35 Å (Fig. 5). The large circular depressions shown in red colours are indicating strong interactions as discussed in the structural description (*vide supra*), whereas the light colour in d_{norm} surfaces are suggesting relatively

weaker interactions (Fig. 5). In the fingerprint plots, the complementary regions can be shown where one molecular moiety acts as donor ($d_e > d_i$) whilst another behaves like an acceptor ($d_e < d_i$). Furthermore, the full fingerprint plots have been de-convoluted to specify the atom pair contacts, which also give percentage contributions of the different interactions existing in the solid state of the molecule. In **Sn-Me**, the N···H/H···N, C···H/H···C and C-O···H/H···O-C contribute 13.9%, 17.6% and 3.9%, respectively to the total Hirshfeld surface area. Likewise, in **Sn-Et**, the N···H/H···N and C···H/H···C contribute 14.9% and 18.2%, respectively to the total Hirshfeld surface area. In both compounds, N···H/H···N interactions appear as pair of discrete spikes of nearly equal lengths in the 2D fingerprint plots in the region between 1.0 Å < ($d_e + d_i$) < 2.3 Å (**Sn-Me**) and 1.1 Å < ($d_e + d_i$) < 2.7 Å (**Sn-Et**). Also, C···H/H···C interactions appear as pair of equal size spikes in the region 0.6 Å < ($d_e + d_i$) < 2.5 Å (**Sn-Me**) and 0.6 Å < ($d_e + d_i$) < 2.7 Å (**Sn-Et**). Apart from these, the C-O···H/H···O-C interactions in **Sn-Me** appears between 1.1 Å < ($d_e + d_i$) < 2.8 Å as pair of equal sized spikes in the total Hirshfeld surface area (Fig. 5).

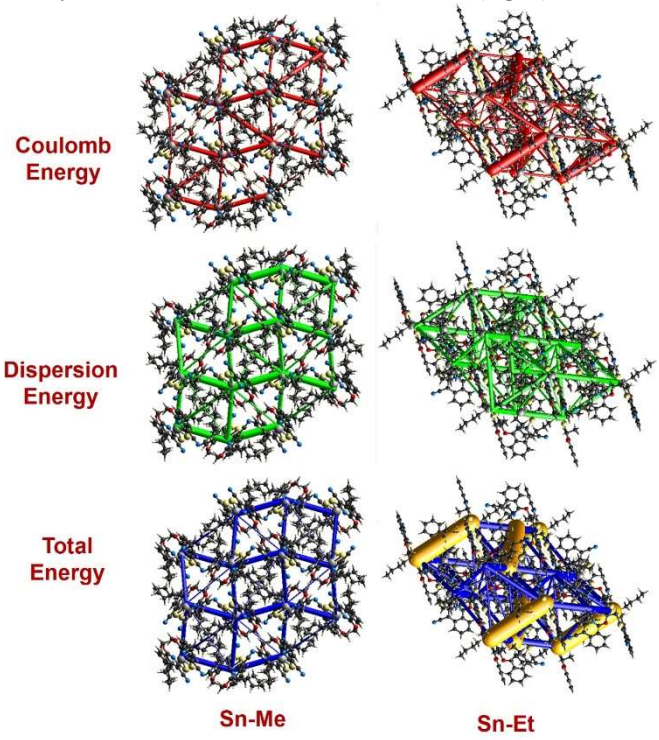

Fig. 6 Pictorial representations of the energy framework calculations for **Sn-Me** and **Sn-Et**.

Furthermore, Crystal Explorer 17.5 was used to compute the interaction energies in a molecular crystal. For this, repulsion, coulomb, dispersion, and total energies for both **Sn-Me** and **Sn-Et** were calculated. These calculations assist in gaining insight into the underlying interaction energy operating between the molecules that lead to the organization of crystal packing into supramolecular architectures in crystalline materials.[23] The molecular environment for both **Sn-Me** and **Sn-Et** were constructed at their center and at distance of ~3.8 Å. The energy benchmarks were calculated in accordance with the Mackenzie's method to scale different energy frameworks, which displayed scale factors for electrostatic, dispersion, polarization, and repulsion of 1.057, 0.740, 0.871, and 0.618, respectively. The relative strengths in interaction energy of molecular packing in all directions displayed cylindrical energy frameworks (Fig. 6). For **Sn-Me**, the polarization, repulsion, and total interaction energies were 89.6 kJ/mol, 275.5 kJ/mol, 326.9 kJ/mol, respectively. While for **Sn-Et**, the calculated polarization, repulsion, and total interaction energies were 91.2 kJ/mol, 281.1 kJ/mol, 332.1 kJ/mol, respectively.

Table 1. Selected topographical features of intermolecular interactions computed at the M06-2X/6-31G**/CEP-121G level of theory for dimeric units of **Sn-Me** and **Sn-Et**.

Interactions	ρbcp	∇2ρbcp	(ε)	H	E (kJ/mol)
Sn-Me					
O1···H30A	+0.0058	+0.0219	+0.0704	0.0009	4.92
C6···H14	+0.0044	+0.0143	+0.4522	0.0012	2.57
N3···H15	+0.0055	+0.0191	+0.0375	0.0009	3.79
N3···H30B	+0.0030	+0.0119	+0.0345	0.0007	1.95
Sn···N2/N4	+0.0196	+0.0351	+0.2834	-0.0015	16.01
Sn-Et					
N1···H1A	+0.0046	+0.0165	+0.3371	0.0009	2.99
N3···H20A	+0.0052	+0.0197	+0.5801	0.0011	3.70
N3···H31A	+0.0076	+0.0243	+0.0485	0.0010	5.45
C11···H3B	+0.0076	+0.0278	+0.7185	0.0015	5.19
C27···H13	+0.0055	+0.0183	+0.4989	0.0011	3.21
Sn···N2/N4	+0.0231	+0.0373	+0.0943	-0.0021	17.92

Computational investigations for non-covalent interaction

Apart from Hirshfeld surface analyses, the weak non-covalent interaction energies in the crystal structure of both **Sn-Me** and **Sn-Et** were computed for two adjacent dimeric units by using the BSSE-corrected M06-2X level of theory. The calculated interaction energies for the dimer of **Sn-Me** held by C···H; N···H and C···H; and O···H interactions are 8.1, 25.9 and 6.9 kJ/mol, respectively. Likewise, in **Sn-Et**, the dimers held by Ar-H···π, and N···H bifurcated and both N···H and C···H interactions possess calculated interaction energies of 8.4, 21.8 and 23.3 kJ/mol, respectively.

Quantum Theory of Atoms in Molecules (QTAIM) analyses were performed to assess the discrete intermolecular interaction energies. The existence of bond critical points (bcp) between the interacting atomic centers are revealed by these calculations, which therefore validate the existence of these non-covalent interactions. The QTAIM calculations suggested that in all type of interactions, the electron density (ρ_{bcp}) between the interacting atom centers is smaller than +0.10 au which indicates that all these interactions are closed shell in nature (Table 1).[24] Also, reduction in electron density between these interacting atom centers are evidenced by the positive Laplacian of the electron density ($\nabla^2\rho_{bcp}$) values for all these interactions (Table 1). Apart from that, the bond ellipticity (ε) which quantifies the extent to which, the electron density is favourably confined the plane of bond path indicated that all these non-covalent interactions are not cylindrically symmetrical.[24] Additionally, weak non-covalent nature of all

these interactions were further confirmed by the total electron energy density (H_b = G + V) suggesting that all these interactions are not accompanied with the substantial sharing of electrons.

Conclusions

To the best of our knowledge this investigation presents for the first time the reaction of di-n-butyltin(IV) dichloride with a dianionic dithiolate ligand derived from 2-(cyanomethyl)benzonitrile which fortuitously yielded 1-methoxy-isoquinoline-4-nitrile thiolate and 1-ethoxy-isoquinoline-4-nitrile thiolate coordinated to di-*n*-butyltin(IV). Here, the dinegative ligand 2-(cyanobenzo)nitrile-dithiolate underwent cyclisation to 1-alkoxy-isoquinoline-4-nitrile thiolates and in presence of two aliphatic alcohols and di-n-butyltin(IV). The obtained newly synthesized compounds displayed peculiar molecular framework and displayed interesting supramolecular architectures using varied non-covalent interactions. These interactions have been further studied using integrated Hirshfeld surface, density functional theory and the quantum theory of atoms-in-molecules approach. Such investigation will upsurge interest amongst the organometallic chemists to utilize main group orgnanometallic precursors to develop analogous systems that can engender interesting supramolecular architectures with tuned properties.

Materials and Methods

General Considerations

All chemical reagents and solvents were obtained from commercial sources and used without further purification. 2-(cyanobenzo)nitrile was obtained from Sigma-Aldrich, KOH and ethanol from Merck, carbon disulfide and methanol from Thermo Fischer Scientific. All solvents were distilled prior to use in accordance with previously reported standard distillation methods. The UV-Vis. spectroscopy for both the compounds were performed on SPECORD 210 PLUS BU UV-Vis. spectrophotometer and elemental analyses were performed using Perkin-Elmer 2400 series II CHNS analyser. Melting point were recorded by employing open capillary method using JSGW melting point apparatus. To record IR spectra Shimadzu IR affinity 1S spectrophotometer was used, while ^{1}H, ^{13}C, ^{119}Sn NMR spectra were recorded on Bruker Avance III HD spectrophotometer. Chemical shifts were recorded in parts per million using TMS as an internal standard for ^{1}H and ^{13}C and tetramethyltin was used as reference for ^{119}Sn NMR spectroscopy as an external standard.

Syntheses

Synthesis of 2-(cyanobenzo)nitrile-dithiolate

The ligand was prepared with slight modification to our previously reported method.[17c] The solution of KOH (0.230 g, 4.10 mmol) in THF was added dropwise into the stirring THF solution of 2-(cyanobenzo) nitrile (0.285 g, 2 mmol) and the yellow solution was stirred for an hour followed by dropwise addition of carbon disulfide (0.200 g, 2.5 mmol). The colour of the reaction mixture turned wine red and the mixture was stirred overnight. The solvent was rotary evaporated and the residue was washed with THF and diethyl ether repeatedly to obtain a dark orange solid that was vacuum dried. Yield: 0.322 g, 55%; m.p. 209-210˚C.

Synthesis of di-*n*-butyltin(IV)-*bis*-(1-methoxy-isoquinoline-4-nitrile thiolate) (Sn-Me)

To a methanol solution (5 mL) of 2-(cyanobenzo)nitrile-dithiolate (0.147 g, 0.5 mmol) was added dropwise the dichloromethane (5 mL) solution of di-*n*-butyltin dichloride (0.155 g, 0.5 mmol) in dropwise manner. The rose red reaction mixture was stirred for 3 h and filtered to obtain a precipitate. The precipitate was washed twice with diethyl ether (2 × 10 mL) dissolved in methanol (5 mL) and left for slow evaporation to obtain pale yellow crystals suitable for single crystal X-ray diffraction.

Yield: 0.143 g, 43.1%; m.p.: 132-135˚C. Elemental analyses calcd., C , 54.31; H, 4.86; N, 8.44; S, 9.87. Found, C , 54.63; H, 4.99; N, 8.98; S, 10.27; IR (KBr, cm^{-1}) *v*: 3269 (Ar ring), 2300 (CN), 1700, 1395, 832, 403. ^{1}H NMR (300 MHz, $CDCl_3$) δ: 8.19 (dd, 2H, J = 7.8 Hz, Ar), 7.91 (dd, 2H, J = 8.1 Hz, Ar), 7.80 (q, 2H, J = 8.5 Hz Ar), 7.55 (s, 2H, Ar), 4.13 (6H, $-OCH_3$), 1.81 (t, 2H, J = 8.3 Hz $-CH_2-$, α-Bu), 1.42 (t, 2H, J = 8.2 Hz $-CH_2-$, β-Bu), 1.25 (q, 2H, J = 8.3 Hz $-CH_2-$, γ-Bu), 0.99 (t, 3H, J = 8.0 Hz $-CH_3$, n-Bu). ^{13}C NMR (75.50 MHz, $CDCl_3$) *δ*: 195.8, 161.3, 134.1, 127.1, 125.5, 126.8, 123.1, 116.7, 55.3, 27.6, 26.4, 26.2, 13.4. ^{119}Sn NMR ($CDCl_3$, 111.94 MHz) *δ*: -137.9.

Characterization Data for *n*-Bu_2SnS:

Yield: 0.113 g, 42.5 %; m.p.: 55-62˚C. ^{1}H NMR (300 MHz, dmso-d_6) *δ*: 1.55 (t, 2H, J = 7.9 Hz, $-CH_2-$, β-Bu), 1.26 (t, 2H, J = 8.0 Hz, Sn-CH_2-, α-Bu), 1.38 (q, 2H, J = 8.3 Hz, $-CH_2-$, γ-Bu), 0.97 (t, 3H, J = 8.0 Hz $-CH_3$, *n*-Bu). ^{13}C NMR (75.50 MHz, dmso-d_6) *δ*: 31.5. 28.4, 26.1, 14.1. ^{119}Sn NMR (111.94 MHz, dmso-d_6) *δ*: -46.30.

Synthesis of di-*n*-butyltin(IV)-*bis*-(1-ethoxy-isoquinoline-4-nitrile thiolate) (Sn-Et)

To ethanol solution (5 mL) of 2-(cyanobenzo)nitrile-dithiolate (0.147 g, 0.5 mmol) was added the dichloromethane (5 mL) solution of di-*n*-butyltin dichloride (0.155 g, 0.5 mmol) in dropwise manner. The rose red reaction mixture was stirred for 3 h and filtered to obtain a precipitate. The precipitate was washed twice with diethyl ether (2 × 10 mL) dissolved in ethanol (5 mL) and left for slow evaporation to obtain light yellow crystals suitable for single crystal X-ray diffraction.

Yield: 0.145 g, 41.9%; m.p.: 141-143˚C. Elemental analyses calcd., C, 55.58; H, 5.25; N, 8.10; S, 9.27. Found, C , 56.18; H, 5.45; N, 8.22; S, 9.98. IR (KBr, cm^{-1})v 3000 (Ar ring), 2946 (Ar ring), 2200 (CN), 1650, 1403, 1326. ^{1}H NMR (300 MHz, $CDCl_3$) *δ*:8.19 (dd, 2H, J = 7.8 Hz, Ar), 7.95 (dd, 2H, J = 8.1 Hz, Ar), 7.88 (q, 2H, J = 8.5 Hz Ar), 7.78 (s, 2H, Ar), 4.52 (q, 4H, J = 7.2 Hz -

OCH_2-), 4.41 (t, 6H, J = 7.2 Hz, -OCH_2CH_3), 1.76 (t, 2H, J = 8.3 Hz -CH_2-, α-Bu), 1.40 (t, 2H, J = 8.2 Hz -CH_2-, β-Bu), 1.26 (q, 2H, J = 8.3 Hz -CH_2-, γ-Bu), 0.98 (t, 3H, J = 8.0 Hz -CH_3, n-Bu). ^{13}C NMR (75 MHz, $CDCl_3$) δ: 194.3, 161.6, 134.4, 127.2, 125.7, 126.9, 123.3, 117.1, 115.3, 55.4, 27.6, 26.6, 26.2, 13.1. ^{119}Sn NMR ($CDCl_3$, 111.94 MHz) δ: -140.2.

Characterization Data for Bu_2SnS

Yield: 0.112 g, 42.6 %; m.p.: 53-65˚C[1] H NMR (300 MHz, dmso-d_6) δ: 1.52 (t, 2H, J = 7.9 Hz, -CH_2-, β-Bu), 1.26 (t, 2H, J = 8.0 Hz, Sn-CH_2-, α-Bu), 1.33 (q, 2H, J = 8.3 Hz, -CH_2-, γ-Bu), 0.96 (t, 3H, J = 8.0 Hz -CH_3, *n*-Bu). ^{13}C NMR (75.50 MHz, dmso-d_6) δ: 31.5. 28.4, 26.1, 14.1. ^{119}Sn NMR (111.94 MHz, dmso-d_6) δ: -46.30.

Synthesis of di-*n*-butyltin(IV)-2-methoxy phenyl acetonitrile dithiolate (2-OMeCN-Sn)

Dichloromethane solution of di-*n*-butyltin (IV) chloride (0.076 g, 0.25 mmol) was added dropwise to the methanol solution of 2-methoxy phenyl acetonitrile dithiolate (0.068 g, 0.25 mmol). The reaction mixture was stirred for 2 h under nitrogen and rotary evaporated. The residue was washed with diethyl ether, dried under vacuum to obtain light yellow residue

Light yellow solid Yield: 0.140 g, 52 % m.p.: 148-153˚C. Elemental analyses calcd.: C, 47.59; H, 5.55; N, 3.08; O, 3.52; S, 14.12; Sn, 26.13. ^{1}H NMR (300 MHz, dmso-d_6) δ: 7.37 (t, 1H, J= 9 Hz, Ar)7.07(d, 1H, J = 8.6 Hz Ar), 6.99 (t, 1H, J = 8 Hz, Ar), 6.94 (s, 1H, J= 6 Hz, Ar), 1.69 (s, 3H, O-CH_3), 1.36 (t, 2H, J = 8.0 Hz , α-Bu), 1.32 (t, 2H, J=7.9Hz, β-Bu), 0.90 (q, 2H, J=7.8 Hz), 0.85 (3H, -CH_3, *n*-Bu). ^{13}C NMR (75.50 MHz, dmso-d_6) δ: 157.1, 130.0, 129.0, 121.0, 119.4, 111.56, 74.6, 56.0, 18.3, 14.2.

X-ray Crystallography

Intensity data for **1** and **2** were collected at 150(2) K on a Rigaku Xcalibur, EosS2 single crystal diffractometer using graphite monochromated Mo-Kα radiation (λ = 0.71073 Å). Unit cell determination, data collection and data reduction were performed using the CrysAlisPro software.[26] The structures were solved with SHELXT[27] and refined by a full-matrix least-squares procedure based on F^2 (SHELXL-2014-16).[27] All non-hydrogen atoms were refined anisotropically. Hydrogen atoms were placed onto calculated positions and refined using a riding model.

Crystal Data for **Sn-Me:** $C_{30}H_{32}N_4O_2S_2Sn$, M = 663.40, Monoclinic $P2_1/c$, a = 12.7211(13) Å, b = 15.4901(11) Å, c = 15.5655(16) Å, β= 106.496(11)°, V=2941.0(5)Å^3 Z=4, DC=1.498 mg.m^3, crystal size 0.300 × 0.280 × 0.200 mm^3, F(000)=1352 reflections collected 21408, independent reflections 5374 [R(int) = 0.0769], Final indices [I> 2σ(I)] R_1 = 0.0654, wR_2 = 0.1257, R indices (all data) R_1 = 0.1203, wR_2 = 0.1502, gof 1.041, Largest difference peak and hole 1.055 and -0.525 e Å^{-3}. **CCDC No.: 2124711**

Crystal Data for **Sn-Et:** $C_{32}H_{36}N_4O_2S_2Sn$, M = 691.46, Monoclinic $P2_1/c$, a = 12.5032 (4) Å, b = 16.2167(5) Å, c = 16.3789 (6) Å, β= 105.745(4)°, V=3196390(19)Å^3 Z=4, D_c=1.437 Mg/m^3, crystal size 0.500 × 0.350 × 0.250 mm^3, F(000)=1416 reflections collected 31507, independent reflections 8499 [R(int) = 0.0400], Final indices [I> 2σ(I)] R_1 = 0.0453, wR_2 = 0.887, R indices (all data) R_1 = 0.0651, wR_2 = 0.0961, gof 1.082, Largest difference peak and hole 0.808 and -0.485 e Å^{-3}. **CCDC No.: 2124712**

Computational details

The gas phase molecular geometries of the monomer as well dimer units of both **Sn-Me** and **Sn-Et** were optimized using density functional theory (DFT) by employing the M06-2X functional.[28] For the C, N, S and H centers, a 6-31G** basis set was used while for Sn LANL2DZ basis sets was employed. To calculate the interaction energy of the dimers held by non-covalent interactions, these interaction distances were fixed and the rest of the degrees of freedom were relaxed during geometry optimization. The stabilization energies (ΔE_{dimer}) for the dimeric entity were calculated using the formula $\Delta E_{dimer} = E_{dimer} - (2 \times E_{monomer})$ where $E_{monomer}$, E_{dimer} are the energies of the monomer and dimer entities, respectively. Since, the non-covalent interactions are considerably weaker than either the ionic or covalent bonding, the basis set superposition error (BSSE) corrections were accounted for during the calculations employing the Boys-Bernardi scheme.[29] All computations have been done using the Gaussian 09 revision B.01 programme.[30]

Hirshfeld Surface Analyses

Molecular Hirshfeld surfaces in the crystal structure of both compounds were constructed by using the procedure mentioned previously. [31-38]

Acknowledgements

AK is obliged to CSIR, New Delhi for the financial support in the form of project no. 01(2899)/17/EMR-II. Dr. Mohd. Muddassir is grateful to Researchers Supporting Project number (RSP-2021/141), King Saud University, Riyadh, Saudi Arabia, for financial assistance.

Conflicts of interest

The authors declare no conflict of interest.

References

1 P. J. Heard, *Prog. Inorg. Chem*. 2005, **53**, 1.
2 D. Coucouvanis, *Prog. Inorg. Chem*., 1970, **11**, 301; (b) G. Hogarth, *Prog. Inorg. Chem*., 2005, **53**, 71.
3 (*a*) J. Cookson, P. D. Beer, *Dalton Trans*., 2007, **15**, 1459-1472; (*b*) E.R.T. Tiekink, I. Haiduc, *Prog. Inorg. Chem*., 2005, **54**, 127-319; (c) T. Okubo, N. Tanaka, K.H. Kim, H. Yone, M. Maekawa, T. Kuroda-Sowa, *Inorg. Chem.*, 2010, **49**, 3700-3702; (*e*) P. I. Clemenson, *Coord. Chem. Rev.,* 1990, **106**, 171-203; (f) E.R.T. Tiekink, *Appl. Organomet. Chem*., 2008, **22**, 533-550.
4 (*a*) R. Chauhan, J. Chaturvedi, M. Trivedi, J. Singh, K.C. Molloy, G. Kociok-Köhn, D. P. Amalnerkar, A. Kumar, *Inorg. Chim. Acta*, 2015, **430**, 168-175; (*b*) R. Chauhan, G. Kociok-Köhn, M. Trivedi, S. Singh, A. Kumar, D. P. Amalnerkar, *J. Solid State Electrochem*., 2015, **19**, 739-747; (*c*) R. Chauhan, M. Trivedi, J. Singh, K.C. Molloy, G. Kociok-Köhn, U.P. Mulik, D.P. Amalnerkar, A. Kumar, *Inorg. Chim. Acta,* 2014, **415**, 69-74; (*d*) A. Kumar, R. Chauhan, K.C. Molloy, G. Kociok-Köhn, L. Bahadur, N. Singh, *Chem. Eur. J.*, 2010, **16**, 4307-4314; (*e*) R. Chauhan, S. Auvinen, A. S. Aditya, M. Trivedi, R.

Prasad, M. Alatalo, D. P. Amalnerkar, A. Kumar, *Sol. Energy*, 2014, **108**, 560-569; (f) D. J. Lewis, P. Kevin, O. Baker, C. A. Muryn, M. A. Malik, P. O'Brien, *Inorg. Chem. Front*., 2014, **1**, 577-598.

5 (*a*) N. Singh, A. Kumar, K. C. Molloy, M. F. Mahon, *Dalton Trans*., 2008, 4999-5007; (*b*) N. Singh, A. Kumar, R. Prasad, K.C. Molloy, M.F. Mahon, *Dalton Trans*., 2010, **39**, 2667; (c) R. Prasad, R. Yadav, M. Trivedi, G. Kociok-Köhn, A. Kumar, *J. Mol. Struct*., 2016, **1103**, 265-270; (*d*) R. Yadav, M. Trivedi, R. Chauhan, R. Prasad, G. Kociok- Köhn, A. Kumar, *Inorg. Chim. Acta,* 2016, **450**, 57–68; (*e*) R. Chauhan, J. Chaturvedi, M. Trivedi, J. Singh, K.C. Molloy, G. Kociok-Köhn, D. P. Amalnerkar, A. Kumar, *Inorg. Chim. Acta,* 2015, **430**, 168–175; (*f*) R. Chauhan, M. Trivedi, R. Yadav, A. Kumar, D. P. Amalnerkar, S. W. Gosavi, *Spectrochim Acta, Part A*: *Mol. Biomol. Spectrosc*., 2015, **150**, 652–656; (*g*) R. Yadav, M. Trivedi, G. Kociok-Köhn, R. Chauhan, A. Kumar, S.W. Gosavi, *Eur. J. Inorg. Chem*., 2016, **2016**, 1013–1021.

6 (*a*) J. O. Adeyemi, D. C. Onwudiwe, E. C. Hoston, J. Mole. Struct., 2019, **1195(5),** 395-402; (*b*) J. O. Adeyemi, D. C. Onwudiwe, N. Nandkumar, M. Singh, De Gruyter(Open Chemistry), 2020, **18(1)**, DOI: 10.1515.chem-2020-0037; (*c*) M. A. Shakban, Z. Xie, N. Savjani, M. A. Malik, P.O' Brien, J. Mater. Sci., 2016, **51**, 6166-6172;(*d*) M. A. Shakban, P. D. Matthews, E. A. Lewis, J. Ratery, I. Vitorica-Yrezabbal, S. J. Haigh, D. L. Lewis, P. O' Brien, *J. Mater. Sci.,* 2019, **54**, 2315-2323; (*e*) J. E. Drake, C. Gurnani, M. Hursthouse, M.Light, M. Nirwan, R. Ratnani, *Appl. Organomet. Chem*., 2007, **21(7)**, 539-544.

7 (*a*) S. F. Kayed, Y. Farina, *J. Saudi Chem. Soc*., 2020, **24(2),** 236-243;(*b*) H. L. Singh, J. B. Singh, S. Bhanuka, *J. Coord. Chem*., 2016, **69(2)**, 343-353;(*c*) M. A. Ali, A. H. Mirza, S. A. Hmaid, P. V. Bernhardt, *Polyhedron*, 2005, **24(3)**, 383-390; (*d*) M. Nath, P. K. Saini *Dalton Trans.*, 2011, **40**, 7077-7121; (*e*) S. Samanta, D. Ghosh, S. Mukopadhyay, A. Endo, T. J. R. Weakley, M. Chaudhury, *Inorg. Chem*., 2003, **42(5)**, 1508-1517.

8 G. Domagk, R. Behnisch, F. Mietzsch, H. Schimidt, *Naturwissenschaften*, 1946, 33,315; (*b*) H. L. Singh, M. Sharma, A. K. Varshney, *Synth. Reac. Inorg. Met. Org. Chem*., 2008, **29(5)**, 817-824; (*c*) M. S. More, P. G. Joshi, Y. K. Mishra, P. K. Khanna, *Material Today Chemistry*, 2019, **14**, 100195; (*d*) M. K. Atal, R. Sharma, A. Saini, V. Dhayal, M. Nagar, *Journal Sol Gel Science and Technology*, 2016, **79**, 114-121.

9 R. Kadu, H. Roy, V.K. Singh, *Appl. Organomet. Chem*., 2015, **29**, 746–755.

10 (*a*) K. Ramasamy, V. L. Kuznetsov, K. Gopal, M. A. Malik, J. Raftery, P. P. Edwards, P. O'Brien, *Chem. Mater.,* 2013, **22,** 266-276; (*b*) J. H. Park, S. G.Kang, Y. K. Lee, T. M. Chung, B. K. Park, C. G. Kim, *Inorg. Chem*., 2020, **59(6)**, 3513-3517; (*c*) C. R. Monzón-González, M. E. Sánchez-Vergara, W. E. Vallejo Narváez, T. Rocha-Rinza, M. Hernández, E. Gómez, O. Jiménez Sandoval, C. Álvarez-Toledano, *Journal Phys. Chem. Solids*, 2021, **50**,109840.

11 (*a*) R.C. Poller, *J. Macromol. Sci.-Chem*., 1978, **12**, 373-378; (*b*) E. Arkis and D. Balkoese, *Polym. Degrad. Stab.,* 2005, **88**, 46-51 (2005).

12 (*a*) R. Devendra, N. R. Edmonds, and T. Söhnel, *J. Mol. Catal. A: Chem*., 2013, 366, 126-139; (*b*) Y. Yuan, Y. Zhang, X. Fu, *RSC Adv.,* 2016, **6,** 83688-83696; (*c*) J. Otera, N. Dan-oh, H. Nozaki, *J. Org. Chem*., 1991, **56**, 5307-5311.

13 (*a*) E. Wlazlak, W. Macyk, W. Nitek, K. Szacilowski, *Inorg. Chem*., 2016, **55**, 5935-5945; (*b*) S. Sanctis, R.C. Hoffmann, M. Bruns, and J. J. Schneider, *Adv. Mater. Interfaces,* 2018*,* **5(15),** 1800324.

14 (*a*) K. Ramasamy, V. L. Kuznetsov, K. Gopal, M. A. Malik, J. Raftery, P. P. Edwards and P. O'Brien, *Chem. Mater*., 2013, **25**, 266-276; (*b*) T. Jiang, G. A. Ozin, *J. Mater. Chem*., 1998, **8**, 1099−1108; (*c*) A. T. Kana, T. G. Hibbert, M. F. Mahon, K. C. Molloy, I. P. Parkin and L. S. Price, *Polyhedron,* 2001, **20**, 2989−2995; (*d*) G. Barone, T. Chaplin, T. G. Hibbert, A. T. Kana, M. F. Mahon, K. C. Molloy, I. D. Worsley, I. P. Parkin and L. S. Price, *J. Chem. Soc., Dalton Trans*., 2013, **2002**, 1085 − 1092; (*e*) M. G. Vasquez-Ríos, V. Reyes-Márquez, H. Höpfl, A. Torres-Huerta, J. Guerrero-Álvarez, M. Sánchez, I. F Hernández-Ahuactzi, K. Ochoa-Lara, A. Jiménez-Sánchez and R. Santillán, *Eur. J. Inorg. Chem*., 2016, **2016**, 3429-3440.

15 (*a*) V. Chandrasekhar, C. Mohapatra, R. J. Butcher, *Cryst. Growth Des*., 2012, **12**, 3285–3295; (*b*) E. Najafi, M.M. Amini, O. Sadeghi, H.R. Khavasi, S.W. Ng, *Heteroatom. Chem*. 2011, **22**, 699–706; (*c*) H. D. Yin, G. Li, Z. J. Gao, H. L. Xu, *J. Organomet. Chem*., 2006, **691**, 1235–1241; (*d*) C. L. Ma, J. K. Li, R. F. Zhang, D. Q. Wang, *Inorg. Chim. Acta,* 2006, **359** 2407– 2416; (*e*) R.G. Xiong, J. L. Zuo, X. Z. You, H.K. Fun, S. Shanmuga, S. Raj, *Organometallics*, 2000, **19**, 4183–4186.

16 (*a*) N. Yang, H. Sun, *Coord. Chem. Rev*., 2007, **251**, 2354–2366; (*b*) V. M. Cangelosi, L. N. Zakharov, D. W. Johnson, *Angew. Chem., Int. Ed*., 2010, **49**, 1248–1251; (*c*) V. M. Cangelosi, T. G. Carter, J. L. Crossland, L. N. Zakharov, and D. W. Johnson, *Inorg. Chem*., 2010, **49**, 9985-9992; (*d*) A. Luqman, V. L. Blair, R. Brammananth, P. K. Crellin, R. L. Coppel, and P. C. Andrews, *Chem. Eur. J*., 2014, **20**, 14362–14377.

17 (*a*) N. Singh, S. Bhattacharya, *J. Organomet. Chem*., 2012, **700**, 69–77; (*b*) A. N. Gupta, V. Kumar, V. Singh, K. K. Mannar, A. K. Singh, M. G. B. Drew, N. Singh, *Polyhedron*, 2015, **787** , 65072; (*c*) R. Yadav, M. Trivedi, G. Kociok-Köhn, R. Prasad, A. Kumar, *CrystEngComm*, 2015, **17**, 9175-9184; (*d*) L. Ombaka, P.G. Ndungu, B. Omandi, V. O Nyaori, *J. Coord. Chem*., 2014, **67(11)**, 1905-1922

18 P. Singh, A. Singh, A. Singh, A. K. Singh, G. Kociok-Köhn, A. Alowais, N. A. Y. Abduh, M. Muddassir and A. Kumar, *CrystEngComm*, 2020, **22**, 2049-2059.

19 (a) J. Holecek, M. Nádvorník, K. Handlíř, A. Lyćka, *J. Organomet. Chem.,* 1986*,* **315**, 299–308; (*b*) M. Hong, G. Chang, R. Li, M. Niu*, New J. Chem*., 2016, **40**, 7889–7900; (*c*) S. Yadav, I. Yousuf, M. Usman, M. Ahmad, F. Arjmand, S. Tabassum, *RSC Adv*., 2015, **5,** 50673–50690.

20 (*a*) R. J. Deeth, K. C. Molloy, M. F. Mahon, S. J. Whittaker, *J. Organomet. Chem.,* 1992, **430**, 25; (*b*) R. Cea-Olivares, O. Jimonez-Sandoval, G. Espinosa-Porez, and C. Silvestru, C., *Polyhedron,* 1994, **13**, 2809-2094; (*c*) R. Cea-Olivares, O. Jimnez-Sandoval, G. Espinosa-Perez, and C. Silvestru, *J. Organomet. Chem*., 1994, **484**, 33-36.

21 (*a*) Z.-U. Rehman, N. Muhammad, S. Shuja, S. Ali, I. S. Butler, A. Meetsma, M. Khan, *Polyhedron,* 2009, **28**, 3439–3448; (*b*) S. Shahzadi, S. Ali, M. Fettouhi, *Acta Crystallogr. sectionI,* 2006*,* **62,** 1178– 1180; (*c*) Z.-U. Rehman, S. Ali, N. Muhammed, A. Meetsma, *Acta Crystallogr. Section* , 2007, **63**, 431–432.

22 (*a*) M. K. Khan, J. Akhtar, M. A. Malik, M. Akhtar, N. Revaprasadu, *New J. Chem*., 2015, 39, 9569–9574; (*b*) A. Kumar , A. Singh , R. Yadav , S. Singh , G. Kociok-Köhn , M. Trivedi, *Inorg. Chim. Acta*, 2018, **471**, 234-243.

23 C. F. Mackenzie, P. R. Spackman, D. Jayatilaka and M. A. Spackman, IUCrJ, 2017, **4**, 575–587.

24 (*a*) C. F. Matta and R. J. Boyd, The Quantum Theory of Atoms in Molecules: From Solid State to DNA and Drug Design; Wiley VCH, VerlagGmbh& Co. KGaA: Germany, 2007; (*b*) C. F. Matta, J. Hernández-Tryjillo, T-H. Tang and R. F. W. Bader, *Chem. Eur. J*, 2003, **9**, 1940-1951.

25 S. Midgal, D. Gertner and A. Zilkha, *Can. J. Chem.*, 1967, **45**, 2987-2992.

26 CrysAlisPro 1.171.40.67a (Rigaku Oxford Diffraction, 2019).

27 G. M. Sheldrick, *Acta Cryst.*, 2015, **C71**, 3–8 and **A71**, 3-8.

28 Y. Zhao and D. G. Truhlar, *Theor. Chem. Acc.*, 2006, **120**, 1-3.

29 S. F. Boys and F. Bernardi, *Mol. Phys.,* 1970, **19**, 553.
30 M. J. Frisch, G. W. Trucks, H. B. Schlegel, G. E. Scuseria, M. A. Robb, J. R. Cheeseman, J. A. Montgomery, T. Vreven Jr., K. N. Kudin, J. C. Burant, J. M. Millam, S. S. Iyengar, J. Tomasi, V. Barone, B. Mennucci, M. Cossi, G. Scalmani, N. Rega, G. A. Petersson, H. Nakatsuji, M. Hada, M. Ehara, K. Toyota, R. Fukuda, J. Hasegawa, M. Ishida, T. Nakajima, Y. Honda, O. Kitao, H. Nakai, M.; Klene, X. Li, J. E. Knox, H. P. Hratchian, J. B. Cross, V. Bakken, C. Adamo, J. Jaramillo, R. Gomperts, R. E. Stratmann, O. Yazyev, A. J. Austin, R. Cammi, C. Pomelli, J. W. Ochterski, P. Y. Ayala, K. Morokuma, G. A. Voth, P. Salvador, J. J. Dannenberg, V. G. Zakrzewski, S. Dapprich, A. D. Daniels, M. C. Strain, O. Farkas, D. K. Malick, A. D. Rabuck, K. Raghavachari, J. B. Foresman, J. V. Ortiz, Q. Cui, A. G. Baboul, S. Clifford, J. Cioslowski, B. B. Stefanov, G. Liu, A. Liashenko, P. Piskorz, I. Komaromi, R. L. Martin, D. J. Fox, T. Keith, M. A. Al-Laham, C. Y. Peng, A. Nanayakkara, M. Challacombe, P. M. W. Gill, B. Johnson, W. Chen, W. M. Wong, C. Gonzalez and J. A. Pople, Gaussian 09 revision B.01, Gaussian, Inc., Wallingford CT, 2009.
31 M. A. Spackman and J. J. McKinnon, *CrystEngComm*, 2002, **4**, 378-392.
32 M. A. Spackman and P. G. Byrom, *Chem. Phy. Lett.*, 1997, **267**, 309.
33 J. J. McKinnon, A. S. Mitchell, and M. A. Spackman, *Chem-Eur. J.*, 1998, **4**, 2136-2141.
34 J. J. McKinnon, M. A. Spackman and A. S. Mitchell, *Acta Crystallogr. Sec. B*, 2004, **60**, 627-668.
35 A. L. Rohl, M. Moret, W. Kaminsky, K. Claborn, J. J. McKinnon and B. Kahr, *Cryst. Growth Des.*, 2008, **8**, 4517-4525.
36 A. Parkin, G. Barr, W. Dong, C. J. Gilmore, D. Jayatilaka, J. J. McKinnon, M. A. Spackman and C. C. Wilson, *CrystEngComm*, 2007, **9**, 648-652.
37 S. K. Wolff, D. J. Greenwood, J. J. McKinnon, D. Jayatilaka and M. A. Spackman, *Crystal Explorer 3.1*; University of Western Australia: Perth, Australia, 2012.
38 J. J. Koenderink and A. J. van Doorn, *Image Vision Comput.* 1992, **10**, 557-564.